

Research Paper

Nonlocal State-Space Strain Gradient Approach to the Vibration of Piezoelectric Functionally Graded Nanobeam

Rajendran SELVAMANI¹*, Rubine LOGANATHAN¹), Farzad EBRAHIMI²)

¹) *Department of Mathematics, Karunya Institute of Technology and Sciences Coimbatore
Tamilnadu, India*

²) *Department of Mechanical Engineering, Imam Khomeini International University
Qazvin, Iran*

*Corresponding Author e-mail: selvam1729@gmail.com

In this work, the state-space nonlocal strain gradient theory is used for the vibration analysis of piezoelectric functionally graded material (FGM) nanobeam. Power law relations are used to describe the computing analysis of FGM constituent properties. The refined higher-order beam theory and Hamilton's principle are used to obtain the equations of motion of the piezoelectric nanobeam. Besides, the governing equations of the piezoelectric nanobeam are extracted by the developed nonlocal state-space theory, and the analytical wave dispersion method is used to solve wave propagation problems. The real and imaginary solutions for wave frequency, loss factor and wave number are obtained and presented in graphs.

Keywords: wave propagation; functionally graded materials (FGMs); nonlocal strain gradient state-space theory; piezoelectric nanobeam.

1. INTRODUCTION

Functionally graded materials (FGMs) are a type of composite materials introduced by a group of Japanese scientists to control the volume fraction of the mixture of two or more materials. KE *et al.* [1] investigated the nonlinear vibration of the piezoelectric nanobeams based on the nonlocal theory and Timoshenko beam theory. The influence of the nonlocal parameter, temperature change and external electric voltage on the size-dependent nonlinear vibration characteristics of the piezoelectric nanobeam were presented. KE and WANG [2] studied the natural frequencies and the thermoelectric-mechanical vibration of piezoelectric nanobeams based on the nonlocal theory. EBRAHIMI *et al.* [3] reported the wave dispersion in viscoelastic FG nanobeam. LAZOPOULOS and LAZOPOULOS [4] dealt with the fractional deformation of a linearly elastic bar.

LAZOPOULOS and LAZOPOULOS [5] studied the fractional bending of beams. ALOTTA *et al.* [6] focused on the finite element formulation of a nonlocal hereditary fractional-order Timoshenko beam. SUMELKA *et al.* [7] studied the fractional Euler-Bernoulli beams. SIDHARDH *et al.* [8] investigated the geometrically nonlinear response of a fractional-order nonlocal model of elasticity. STEMPIN and SUMELKA [9] established the space fractional Euler-Bernoulli beam model.

OSKOUIE *et al.* [10] considered the bending analysis of functionally graded nanobeam based on the fractional nonlocal continuum theory using the variational Legendre spectral collocation method. Stress-driven model versus strain-driven nonlocal integral model for elastic nanobeams was discussed by ROMANO and BARRETTA [11]. The structural behavior of FG nanobeams under stress-driven and strain-driven integral elasticity was studied by BARRETTA *et al.* [12]. A stability investigation was performed and the internal length effect was obtained by analyzing the critical eigenspace by BEDA [13]. The free vibration and buckling of a Timoshenko nano-beam using the Eringen generalized theory based on the fractional derivatives were studied by MOHAMMADI *et al.* [14]. NGUYEN *et al.* [15] studied the free vibration of thin-walled FG open-section beams. EBRAHIMI and BARATI [16] investigated the vibration characteristics of magneto-electro-thermo-elastic functionally graded (METE-FG) nanobeams within the framework of third-order shear deformation theory. ZAOUI *et al.* [17] dealt with the free vibrations of FG nanoplates resting on an elastic foundation using the Hamilton principle. ALIBEIGI *et al.* [18] introduced the buckling response of nanobeams based on the Euler-Bernoulli beam model with the von Kármán geometrical nonlinearity. SHARIATI *et al.* [19] focused on the bending of flexo-electric magneto-electro-elastic (MEE) nanobeams lying over the Winkler-Pasternak foundation according to nonlocal elasticity theory. EBRAHIMI *et al.* [20] presented bending analysis of magneto-electro-elastic nanobeams system under hygro-thermal loading. EBRAHIMI and DABBAGH [21] tested the dynamic analysis of smart nanostructures.

LI *et al.* [22] considered tri-stimuli thermo-electro-mechanical constitutive modeling for the frequency analysis of statically thermal postbuckled FGM thin beams. KIANI and ESLAMI [23] discussed the nonlinear buckling temperature of FGM beams using kinematic modeling. SUN and LUO [24] reported the wave propagation of FG material plates in thermal environments. THAI and CHOI [25] presented a consistent and refined higher-order shear deformation theory (HSDT) to probe the modal characteristics of FGM thick plates seated on a stiff substrate. Using a new parabolic HSDT, vibrational responses of FGM thick plates were studied by THAI *et al.* [26]. SHAHSAVARI *et al.* [27] investigated the influences of voids in the FGM on the natural frequencies of composite plates based on a quasi-3D plate model.

From then on, many attempts were carried out to analyze the responses of nanosized elements subjected to different working conditions. To predict the mechanical behaviors of nanostructures, the constitutive behaviors of such structures cannot be assumed to be the same as those of macroscale structures. The first effort in this field was performed in the context of the nonlocal elasticity by ERINGEN [28]. The bending analysis of microtubules using the Euler-Bernoulli beam theory was reported by CIVALEK and DEMIR [29]. Implementing the nonlocal theory of elasticity for piezoelectric nanotubes by conveying a flow of viscous fluid, a nonlinear buckling load of smart boron nitride nanoshells supported by a bundle of carbon nanotubes (CNTs) was investigated in [30]. Concentrating on the nanobeams made from bi-directional FGMs, the bending, buckling, and vibration characteristics of such nonlocal elements were reported in [30] by Eringen's scale-dependent model. ARANI *et al.* [30] used the classical and first-order beam hypotheses to find the finite element nonlinear bending models in nanobeams. Nonlocal and surface elasticity theories were merged by REDDY and EL-BORGI [31] to probe the effects of surface stresses on the dispersion of waves in smart piezoelectric nanoplates. Concentrating on the nanobeams made from bi-directional FGMs, bending, buckling, and vibration characteristics of such nonlocal elements were reported in NEJAD and HADI [33, 34] by Eringen's scale-dependent model. EBRAHIMI and BARATI [36] used the nonlocal theory to survey the natural frequency's variation in nanocrystalline nanobeams located on a viscoelastic sheet. By considering size-dependent elements of the beam, the bending properties of such tiny elements were analyzed in the context of the nonlocal theory and the Timoshenko model of moderately thick beams by EBRAHIMI and BARATI [36]. Regarding this issue and preserving the basic assumptions of the nonlocal elasticity, the nonlocal stress-strain gradient elasticity was discussed by LIM *et al.* [37]. Like nonlocal elasticity, nonlocal strain gradient theory (NSGT) has been used broadly in recent years to analyze the mechanical characteristics of nanostructures. Based on this advanced theory, the thermo-mechanical buckling problem of graphene sheets was analyzed by FARAJPOUR *et al.* [38]. The modal characteristics of FGM nanobeams were studied by LI *et al.* [39]. The combination of NSGT and surface elasticity for smart piezoelectric solids was accomplished by EBRAHIMI and DABBAGH [40], and its application in solving the wave dispersion problem in nanoplates was presented. Moreover, the vibrational responses of nanobeams manufactured from FGMs with 3D-graded properties were investigated in [41] by NSGT.

Hence this work presents the wave propagation analysis of FGM piezoelectric nanobeam with the help of a nonlocal state-space strain gradient viscoelasticity. The constituent properties of FGM are implemented via power law relations, and the motion of equations is derived through Hamilton's principle. Furthermore,

the dispersion for computed wave frequency, loss factor and wave number are presented and discussed for real and imaginary modes of vibration.

2. PROBLEM FORMULATION

This study investigates a viscoelastic FG nanobeam of length L , width b , and thickness h based on the state-space nonlocal strain gradient theory. The constituent FGM consists of two parts: a ceramic part that is made of Si_3N_4 and a metallic part that is made of SUS304. To develop a more realistic viscoelastic study, the material properties of the FGM's constituents are presumed to be temperature sensitive. In this section, power-law relations are used to compute the properties. The volume fraction of each phase needs to be calculated to calculate these temperature variable properties in the thickness direction, and according to the power law model, the volume fraction of the ceramic part is calculated:

$$(2.1) \quad V_c = \left(\frac{z}{h} + \frac{1}{2} \right)^p,$$

where h is the thickness of the structure, z is the distance from the neutral plane of the FG beam, and p is the power law exponent examining the distribution of properties of each phase in the material. It must be considered that any desired material property can be related to the local temperature as:

$$(2.2) \quad P = P_0 (P_{-1}T^{-1} + 1 + P_1T + P_2T^2 + P_3T^3),$$

where $P_0, P_{-1}, P_1, P_2, P_3$ are the coefficients of material phases.

The volume fraction of the metallic phase gives the volume fraction of the ceramic phase by $V_m = 1 - V_c$.

The material properties of nonlocal FGM, including Young's modulus (E), mass density (ρ), and Poisson's ratio (ν) are as follows:

$$(2.3) \quad \begin{aligned} E(z) &= E_c V_c + E_m V_m, \\ \rho(z) &= \rho_c V_c + \rho_m V_m, \\ \nu(z) &= \nu_c V_c + \nu_m V_m. \end{aligned}$$

To obtain the governing equations of the problem, a precise kinematic theory for nanobeams is used. The effects of shear strain and stress on the deflection of thick-type structures are included in HSDT. The displacement field of the refined shear deformable beam can be expressed by [8]:

$$(2.4) \quad \begin{aligned} U_x(X, Z, t) &= U(X, t) - Z \frac{\partial w_b(X, t)}{\partial X} - f(Z) \frac{\partial w_s(X, t)}{\partial X}, \\ U_z(X, Z, t) &= w_b(X, t) + w_s(X, t), \end{aligned}$$

where U_x , U_z denote the longitudinal displacement, and the bending and shear components of the transverse displacement are shown with w_b and w_s , respectively. Also, the distribution of shear strain in the direction of beams thickness is the shape function that determines $f(z)$ [4]:

$$(2.5) \quad f(z) = \frac{he^z}{h^2 + \pi^2} \left[\pi \sin\left(\frac{\pi z}{h}\right) + h \cos\left(\frac{\pi z}{h}\right) \right] - \frac{h^2}{h^2 + \pi^2}.$$

The distorted cross-section of the structure will be approximated with this function to capture the shear strain and stress. This function is also responsible for satisfying the assumption of the nonexistence of shear strain at free surfaces.

By continuum infinitesimal strain tensor, the nonzero strains can be modeled as:

$$(2.6) \quad \begin{aligned} \varepsilon_{xx} &= \frac{\partial u}{\partial x} - z \frac{\partial^2 w_b}{\partial x^2} - f(z) \frac{\partial^2 w_s}{\partial x^2}, \\ \gamma_{xz} &= g(z) \frac{\partial w_s}{\partial x}, \end{aligned}$$

where

$$g(z) = 1 - \frac{df(z)}{dz}$$

2.1. Motion equations

In the purview of Hamilton's principle, the Lagrangian change of the system will be zero, and the extended Lagrangian is:

$$(2.7) \quad L = U - T + V,$$

so, Hamilton's principle is expressed as:

$$(2.8) \quad \delta \int_{t_1}^{t_2} (U - T + V) dt = 0.$$

In Eq. (2.8), the strain energy is U and the work done by external force is V . Also, T stands for kinetic energy. The virtual strain energy can be written as:

$$(2.9) \quad \delta U = \int_A (\sigma_{ij} \delta \varepsilon_{ij} - D_x \delta E_x - D_z \delta E_z) dA,$$

$$(2.10) \quad \phi(x, z, t) = -\cos(\beta z) \phi(xt) + \frac{2zV_0}{h} e^{-i\Omega t},$$

where $\beta = \frac{\pi}{h}$, $\phi(x, t)$ is the variation of electric potential in the x direction, V_0 is the external electric voltage, and Ω is the natural frequency of the piezoelectric nanobeam.

By introducing Eq. (2.6) in Eq. (2.9):

$$(2.11) \quad \delta U = \int_0^L \int_{-\frac{h}{2}}^{\frac{h}{2}} \left(N \frac{\partial \delta U}{\partial x} - M_b \frac{\partial^2 \delta w_b}{\partial x^2} - M_s \frac{\partial^2 \delta w_s}{\partial x^2} + Q \frac{\partial \delta w_s}{\partial x} - D_x \delta E_x - D_z \delta E_z \right) dz dx,$$

the stress resultants can be obtained as:

$$(2.12) \quad [N, M_b, M_s] = \int_A [1, z, f(z)] \sigma_{xx} dA,$$

$$(2.13) \quad Q = \int_A g(z) \sigma_{xz} dA.$$

The variation of the system's kinetic energy is as follows:

$$(2.14) \quad \delta T = \int_A \rho(z) \left[\frac{\partial u_x}{\partial t} \frac{\partial \delta u_x}{\partial t} + \frac{\partial u_z}{\partial t} \frac{\partial \delta u_z}{\partial t} \right] dA.$$

Substitution of Eq. (2.4) in Eq. (2.14) produces

$$(2.15) \quad \delta T = \int_0^L \int_{-\frac{h}{2}}^{\frac{h}{2}} \left[I_0 \left(\frac{\partial u}{\partial t} \frac{\partial \delta u}{\partial t} + \frac{\partial (w_b + w_s)}{\partial t} \frac{\partial \delta (w_b + w_s)}{\partial t} \right) - I_1 \left(\frac{\partial u}{\partial t} \frac{\partial^2 \delta w_b}{\partial x \partial t} + \frac{\partial^2 w_b}{\partial x \partial t} \frac{\partial \delta u}{\partial t} \right) - J_1 \left(\frac{\partial u}{\partial t} \frac{\partial^2 \delta w_s}{\partial x \partial t} + \frac{\partial^2 w_s}{\partial x \partial t} \frac{\partial \delta u}{\partial t} \right) + I_2 \frac{\partial^2 w_b}{\partial x \partial t} \frac{\partial^2 \delta w_b}{\partial x \partial t} + K_2 \frac{\partial^2 w_s}{\partial x \partial t} \frac{\partial^2 \delta w_s}{\partial x \partial t} + J_2 \left(\frac{\partial^2 w_b}{\partial x \partial t} \frac{\partial^2 \delta w_s}{\partial x \partial t} + \frac{\partial^2 w_s}{\partial x \partial t} \frac{\partial^2 \delta w_b}{\partial x \partial t} \right) \right] dz dx,$$

where mass moments of inertia used in the definition (2.15) can be defined as:

$$(2.16) \quad [I_0, I_1, I_2, J_1, J_2, K_2] = \int_A [1, z, z^2, f(z), z f(z), f^2(z)] \rho(z) dA.$$

To obtain the Euler–Lagrange equations of the beam, Eqs. (2.11) and (2.15) must be inserted in Eq. (2.8), and the outcome must be coupled as:

$$(2.17) \quad \frac{\partial N}{\partial x} = I_0 \frac{\partial^2 u}{\partial t^2} - I_1 \frac{\partial^3 w_b}{\partial x \partial t^2} - J_1 \frac{\partial^3 w_s}{\partial x \partial t^2},$$

$$(2.18) \quad \frac{\partial^2 M_b}{\partial x^2} = I_0 \frac{\partial^2 (w_b + w_s)}{\partial t^2} + I_1 \frac{\partial^3 u}{\partial x \partial t^2} - I_2 \frac{\partial^4 w_b}{\partial x^2 \partial t^2} - I_2 \frac{\partial^4 w_s}{\partial x^2 \partial t^2},$$

$$(2.19) \quad \frac{\partial^2 M_b}{\partial x^2} + \frac{\partial Q}{\partial x} = I_0 \frac{\partial^2 (w_b + w_s)}{\partial t^2} + J_1 \frac{\partial^3 u}{\partial x \partial t^2} - J_2 \frac{\partial^4 w_b}{\partial x^2 \partial t^2} - K_2 \frac{\partial^4 w_s}{\partial x^2 \partial t^2},$$

$$(2.20) \quad \delta\phi = \int_{-\frac{h}{2}}^{\frac{h}{2}} \left[\cos(\beta z) \left(\frac{\partial dx}{\partial x} \right) + \beta \sin(\beta z) \right] dz.$$

3. NONLOCAL STATE-SPACE CONSTITUTIVE EQUATIONS

In this section, we demonstrated that both stress and strain are greatly influenced by the nonlocal phenomena in both temporal and spatial domains whenever excitation frequency or wavelength interferes with the intrinsic characteristic length and time. A combination of the Boltzmann superposition integral and the concept of the nonlocal elasticity of Eringen was the foundation of the nonlocal time-space viscoelasticity problems. Through this, the stress and strain tensors of any desired nanostructure are expressed in the framework of convolution functions that can be related to each other with regard to a coupling between temporal and spatial characteristic parameters.

Accordingly, the most general state of the nonlinear integral stress and strain relationship are in the form of the following equation:

$$(3.1) \quad \int_{-\infty}^t \int_v K_\sigma (|r - r'|, t - \tau) \sigma_{ij} (r', \tau) dr' d\tau \\ = \int_{-\infty}^t \int_v K_\varepsilon (|r - r'|, t - \tau) C_{ijkl} \varepsilon_{kl} (r', \tau) dr' d\tau,$$

where σ_{ij} and ε_{kl} are the corresponding arrays of stress and strain tensors, respectively, and C_{ijkl} are the elastic constants. Also, $K_\sigma (|r - r'|, t - \tau)$ and $K_\varepsilon (|r - r'|, t - \tau)$ are the nonlocal kernel functions used. Based on a bi-step Fourier transformation followed by its inversion and implementation of the Taylor series, Eq. (3.1) can be reduced to the following time-space nonlocal viscoelasticity constitutive relation:

$$(3.2) \quad \left(1 - l_\sigma^2 \nabla^2 + \tau_\sigma \frac{\partial}{\partial t} \right) \sigma_{ij} = C_{ijkl} \left(1 - l_\varepsilon^2 \nabla^2 + \tau_\varepsilon \frac{\partial}{\partial t} \right) \varepsilon_{kl}.$$

However, the model (3.2) can cover the spatial nonlocality in a softening manner and the influences of stiffness-hardening are not included in it. To compen-

sate, the concept of the nonlocal strain gradient elasticity must be incorporated into the equation. A simple mathematical manipulation is carried out and the nonlocal strain gradient viscoelasticity is obtained:

$$(3.3) \quad \left(1 - l_\sigma^2 \nabla^2 + \tau_\sigma \frac{\partial}{\partial t}\right) \sigma_{ij} = C_{ijkl} \left(1 - l_\varepsilon^2 \nabla^2 + \tau_\varepsilon \frac{\partial}{\partial t}\right) \varepsilon_{kl}.$$

The Kelvin-Voigt three-parameter model in a solid state viscoelastic material is given by:

$$(3.4) \quad (1 - \mu^2 \nabla^2) \sigma_{ij} = C_{ijkl} \left(1 - \lambda^2 \nabla^2 + \tau \frac{\partial}{\partial t}\right) \varepsilon_{kl}.$$

In relation (3.4), $\mu = l_\sigma$ and $\lambda = l_\varepsilon$ are nonlocal and length scale parameters, respectively. The nonlocal parameter will be considered to be a product of the nanostructure's thickness to include the influences of the characteristic length of the continuous system. To relate the rheological behavior of the system to its spatial nonlocality, the relation between μ and τ will be considered to be $\tau = \mu(\tau_c/E_c)^{1/2}$. The stress resultants may be connected to the components of the structure's displacement field after the foregoing definition is integrated over the cross-section area of the nanobeam with regard to the definition stated in Eqs. (2.12) and (2.13):

$$(3.5) \quad (1 - \mu^2 \nabla^2) N = \left(1 - \lambda^2 \nabla^2 + \tau \frac{\partial}{\partial t}\right) \cdot \left(A_{xx} \frac{\partial u}{\partial x} - B_{xx} \frac{\partial^2 w_b}{\partial x_2} - B_{xx}^s \frac{\partial^2 w_s}{\partial x_2}\right) - e_{31} E_z,$$

$$(3.6) \quad (1 - \mu^2 \nabla^2) M^b = \left(1 - \lambda^2 \nabla^2 + \tau \frac{\partial}{\partial t}\right) \cdot \left(B_{xx} \frac{\partial u}{\partial x} - D_{xx} \frac{\partial^2 w_b}{\partial x_2} - D_{xx}^s \frac{\partial^2 w_s}{\partial x_2}\right) - e_{31} E_z,$$

$$(3.7) \quad (1 - \mu^2 \nabla^2) M^s = \left(1 - \lambda^2 \nabla^2 + \tau \frac{\partial}{\partial t}\right) \cdot \left(B_{xx}^s \frac{\partial u}{\partial x} - D_{xx}^s \frac{\partial^2 w_b}{\partial x_2} - H_{xx}^s \frac{\partial^2 w_s}{\partial x_2}\right) - e_{31} E_z,$$

$$(3.8) \quad (1 - \mu^2 \nabla^2) Q^{xz} = \left(1 - \lambda^2 \nabla^2 + \tau \frac{\partial}{\partial t}\right) \left(A_{xx}^s \frac{\partial w_s}{\partial x}\right) - e_{15} E_x,$$

$$(3.9) \quad (1 - \mu^2 \nabla^2) D_x = e_{15} \gamma_{xz} + e_{11} E_x,$$

$$(3.10) \quad (1 - \mu^2 \nabla^2) D_z = e_{31} \varepsilon_{xx} + e_{33} E_z,$$

where cross-sectional rigidities are:

$$(3.11) \quad [A_{xx}, B_{xx}, B_{xx}^s, D_{xx}, D_{xx}^s, H_{xx}^s] = \int_A [1, z, f(z), z^2, zf(z), f^2(z)] dA,$$

$$(3.12) \quad A^s = \int_A g^2(z)G(z) dA.$$

4. GOVERNING EQUATIONS

Equations (3.5)–(3.10) must be substituted into Eqs. (2.17)–(2.20). Now the nonlocal state-space strain gradient-based governing equations are

$$(4.1) \quad \left(1 - \lambda^2 \nabla^2 + \tau \frac{\partial}{\partial t}\right) \left(A_{xx} \frac{\partial^2 u}{\partial x^2} - B_{xx} \frac{\partial^3 w_b}{\partial x^3} - B_{xx}^s \frac{\partial^3 w_s}{\partial x^3}\right) \\ + (1 - \mu^2 \nabla^2) \left(-I_0 \ddot{u} + I_1 \frac{\partial \ddot{w}_b}{\partial x} + J_1 \frac{\partial \ddot{w}_s}{\partial x}\right) - e_{31} E_z = 0,$$

$$(4.2) \quad \left(1 - \lambda^2 \nabla^2 + \tau \frac{\partial}{\partial t}\right) \left(B_{xx} \frac{\partial^3 u}{\partial x^3} - D_{xx} \frac{\partial^4 w_b}{\partial x^4} - D_{xx}^s \frac{\partial^4 w_s}{\partial x^4}\right) \\ + (1 - \mu^2 \nabla^2) \left(-I_0 (\ddot{w}_b + \ddot{w}_s) - I_1 \frac{\partial \ddot{u}}{\partial x} + I_2 \frac{\partial^2 \ddot{w}_b}{\partial x^2} + J_2 \frac{\partial^2 \ddot{w}_s}{\partial x^2}\right) - e_{31} E_z = 0,$$

$$(4.3) \quad \left(1 - \lambda^2 \nabla^2 + \tau \frac{\partial}{\partial t}\right) \left(B_{xx}^s \frac{\partial^3 u}{\partial x^3} - D_{xx}^s \frac{\partial^4 w_b}{\partial x^4} - H_{xx}^s \frac{\partial^4 w_s}{\partial x^4} + A^s \frac{\partial^2 w_s}{\partial x^2}\right) \\ + (1 - \mu^2 \nabla^2) \left(-I_0 (\ddot{w}_b + \ddot{w}_s) - J_1 \frac{\partial \ddot{u}}{\partial x} + J_2 \frac{\partial^2 \ddot{w}_b}{\partial x^2} + K_2 \frac{\partial^2 \ddot{w}_s}{\partial x^2}\right) \\ - e_{31} E_z - e_{15} E_x = 0.$$

5. ANALYTICAL SOLUTION

This section aims to solve equations obtained in Sec. 4. Here, the analytical wave dispersion method is used to solve wave propagation problems of various types of structures including beams, plates and shells. The solution function of a higher-order beam is

$$(5.1) \quad \begin{Bmatrix} u \\ w_b \\ w_s \end{Bmatrix} = \begin{Bmatrix} U \exp[i(\beta x - \omega t)] \\ w_b \exp[i(\beta x - \omega t)] \\ w_s \exp[i(\beta x - \omega t)] \end{Bmatrix},$$

where the unknown amplitudes of wave propagation are U , w_b , and w_s . The circular frequency and the wave number of the dispersed waves are ω and β , respectively. By substituting the expression (5.1) into Eqs. (4.1)–(4.3), we obtain:

$$(5.2) \quad \{[K] + [C]\omega + [M]\omega^2\} \begin{Bmatrix} U \\ w_b \\ w_s \end{Bmatrix} = 0,$$

where $[K]$, $[C]$, and $[M]$ are the stiffness, damping, and mass matrices, respectively. The components of these symmetric matrices are

$$(5.3) \quad \begin{aligned} k_{11} &= -(1 + \lambda^2\beta^2) A_{xx}\beta^2, \\ k_{12} &= i(1 + \lambda^2\beta^2) B_{xx}\beta^3, \\ k_{13} &= i(1 + \lambda^2\beta^2) B_{xx}^s\beta^3, \\ k_{14} &= e_{31}(1 - \lambda^2\beta^2)\beta \sin(\beta z)\phi - \frac{2V_0e^{i\Omega t}}{h}, \\ k_{22} &= -(1 + \lambda^2\beta^2) D_{xx}\beta^4, \\ k_{23} &= -(1 + \lambda^2\beta^2) D_{xx}^s\beta^4, \\ k_{24} &= e_{31}(1 - \lambda^2\beta^2)\beta \sin(\beta z)\phi - \frac{2V_0e^{i\Omega t}}{h}, \\ k_{33} &= -(1 + \lambda^2\beta^2) (H_{xx}^s\beta^4 + A^s\beta^2), \\ k_{34} &= e_{31}(1 - \lambda^2\beta^2)\beta \sin(\beta z)\phi - \frac{2V_0e^{i\Omega t}}{h}, \end{aligned}$$

$$(5.4) \quad \begin{aligned} c_{11} &= -A_{xx}\tau\beta^2, \\ c_{12} &= iB_{xx}\tau\beta^3, \\ c_{13} &= iB_{xx}^s\tau\beta^3, \\ c_{14} &= \tau e_{31} \left(\beta^2 \cos(\beta z) \frac{dz}{dt} \phi - \left(\frac{2V_0e^{i\Omega t}}{h} (i\Omega) \right) \right), \\ c_{22} &= -D_{xx}\tau\beta^4, \\ c_{23} &= -D_{xx}^s\tau\beta^4, \\ c_{24} &= \tau e_{31} \left(\beta^2 \cos(\beta z) \frac{dz}{dt} \phi - \left(\frac{2V_0e^{i\Omega t}}{h} (i\Omega) \right) \right), \\ c_{33} &= -\tau\beta^2 (H_{xx}^s\beta^2 + A_s), \\ c_{34} &= \tau e_{31} \left(\beta^2 \cos(\beta z) \frac{dz}{dt} \phi - \left(\frac{2V_0e^{i\Omega t}}{h} (i\Omega) \right) \right), \end{aligned}$$

$$\begin{aligned}
 m_{11} &= -(1 + \mu^2 \beta^2) I_0, \\
 m_{12} &= i\beta(1 + \mu^2 \beta^2) I_1, \\
 m_{13} &= i\beta(1 + \mu^2 \beta^2) J_1, \\
 m_{22} &= -(1 + \mu^2 \beta^2)(I_0 + I_2 \beta^2), \\
 m_{23} &= -(1 + \mu^2 \beta^2)(I_0 + J_2 \beta^2), \\
 m_{33} &= -(1 + \mu^2 \beta^2)(I_0 + K_2 \beta^2).
 \end{aligned}
 \tag{5.5}$$

6. RESULTS AND DISCUSSION

In this section, Table 1 shows the considered material phase coefficients for the constituent materials Si_3N_4 and SUS304, which was discussed by EBRAHIMI *et al.* [3]. Table 2 gives the material property of the piezoelectric PZT-4 with its constituent properties [1]. Table 3 shows the comparison of the buckling load for the various power-law exponent values. In Table 3, we see a consistent agreement of the physical variables with the literature (NGUYEN *et al.* [15]).

Table 1. Material properties of Si_3N_4 and SUS304 [3].

Material	Property	P_0	P_{-1}	P_1	P_2	P_3
Si_3N_4	E [Pa]	348.43e9	0	$-3.070e^{-4}$	$2.160e^{-7}$	$-8.946e^{-11}$
	ρ [kg/m ³]	2370	0	0	0	0
	ν [-]	0.24	0	0	0	0
SUS304	E [Pa]	201.04e9	0	$-3.070e^{-4}$	$-6.534e^{-7}$	0
	ρ [kg/m ³]	8166	0	0	0	0
	ν [-]	0.3262	0	$-2.002e^{-4}$	$3.797e^{-7}$	0

Table 2. Material property of PZT-4 [1].

PZT-4	e_{31} [c/m ²]	e_{11} [c/Vm]	e_{33} [N/m ² K]	e_{15} [c/m ²]
	-4.1	$5.841 \cdot 10^{-9}$	$7.124 \cdot 10^{-9}$	14.1

Table 3. Comparison of the non-dimensional buckling load of FGM beam for various power-law exponents [15].

L/h		$p = 0$	$p = 0.5$	$p = 1$	$p = 2$	$p = 5$	$p = 10$
5	NGUYEN <i>et al.</i> [15]	48.8406	32.0013	24.6894	19.1577	15.7355	14.1448
	Present	48.835	31.967	24.6870	19.1605	15.7401	14.13
10	NGUYEN <i>et al.</i> [15]	52.3083	34.0002	26.1707	20.3909	17.1091	15.5278
	Present	52.3082	34.0087	26.1727	20.3936	17.1118	15.5291

As illustrated in Figs. 1a and 1b, the correlation of wave frequency to wave number for an actual and an imaginary mode without piezo effect is shown, and an increasing real value is observed when the wave frequency shoots up, whereas the imaginary value gradually increases gradually with the tip value of 3.8 for the increasing wave frequency.

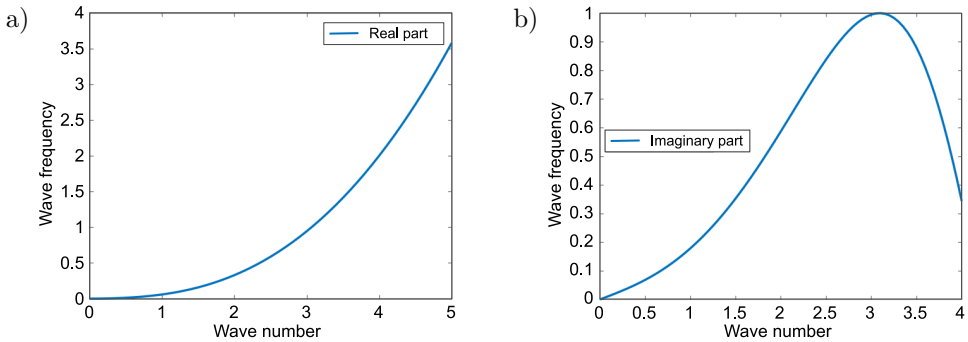


FIG. 1. Variation of wave frequency versus wave number for real (a) and imaginary (b) modes without piezo effect.

Figure 2 shows the plots of real and imaginary modes when the wave frequency is against the wave number. Hence, it is noted that the real and imaginary modes increase gradually up to some wave number value after 3.0. Figure 3 exhibits the real and imaginary modes with the variation of wave frequency against wave number influenced by the piezo effect.

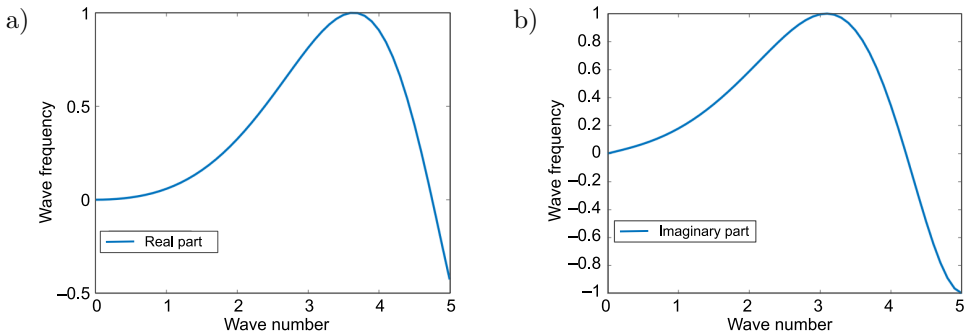


FIG. 2. Variation of wave frequency against wave number for real (a) and imaginary (b) modes with piezo effect.

According to Fig. 4, the raising mode of the real and imaginary scenarios reaches the tip at 3.8 and 3.0, respectively. The variation of wave frequency against wave number for real and imaginary modes without the effect of electric voltages is plotted and shows a gradual linear increment of 3.8 for the real mode and the tip value of 3.0 for the imaginary mode.

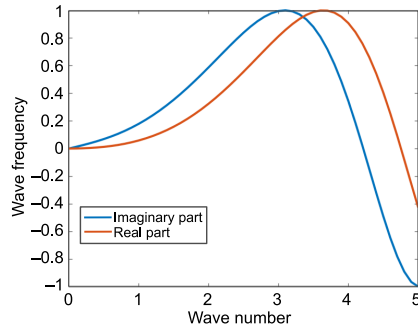


FIG. 3. Variation of wave frequency against wave number in both real and imaginary modes with piezo effect.

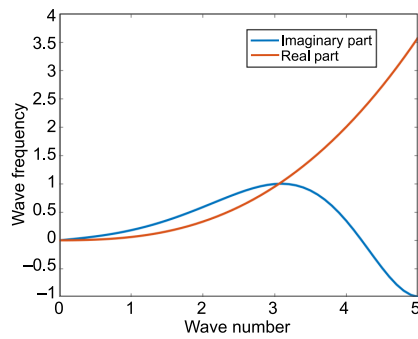


FIG. 4. Variation of wave frequency against wave number for real and imaginary modes without piezo effect.

The variation of electric voltage is presented in Fig. 5. Hence, the electric voltages $V_0 = 0.00$, 0.05 , and 0.5 show an increasing linear effect if the wave number also increases against the wave frequency. Figure 6 shows a variation of loss factor against wave frequency for various V_0 . It is shown that when the given electric voltages $V_0 = 0.005$, 0.05 , and 0.5 are plotted, a dynamic variation of loss factor against wave frequency is observed.

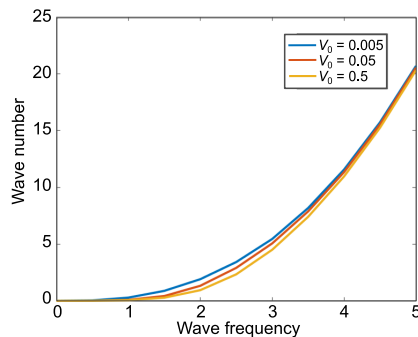


FIG. 5. Variation of wave number against wave frequency for various V_0 .

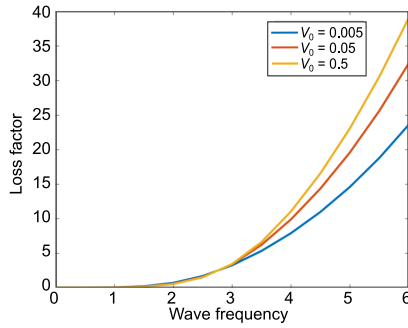


FIG. 6. Variation of loss factor against wave frequency for various V_0 .

Figure 7 shows the relation between the loss factor against nonlocal e_0 for different β . Figure 8 shows the relation between the loss factor against wave frequency in accordance with the nonlocal values μ and it is found that by increasing the wave frequency, the loss factor also increases, and the influence of non-local values on the loss factor is noticeable.

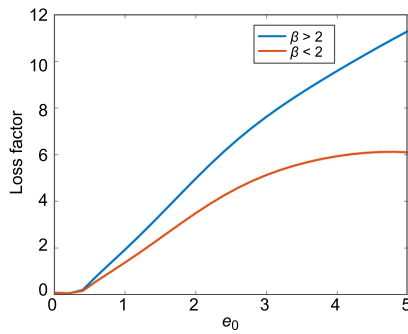


FIG. 7. Variation of loss factor against e_0 for different β .

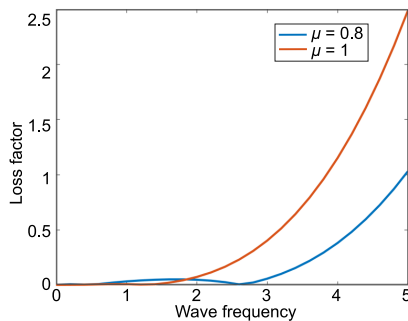


FIG. 8. Variation of loss factor against wave frequency for different μ .

Figure 9 shows that if $\beta = 1$, the loss factor against the wave frequency increases gently in a linear manner, and if $\beta = 1.5$ then it shoots up to 4.5.

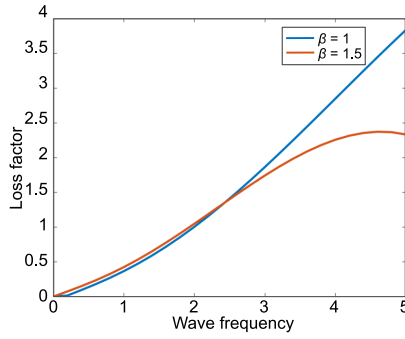


FIG. 9. Variation of loss factor against wave frequency for different β .

Figure 10 exhibits a variation of loss factor against wave frequency with different nonlocal e_0 values. When $e_0 = 0.6$, the loss factor increases at $\omega = 4$ and then reduces gradually. If $e_0 = 0.8$ there is a notable increment after 2.8.

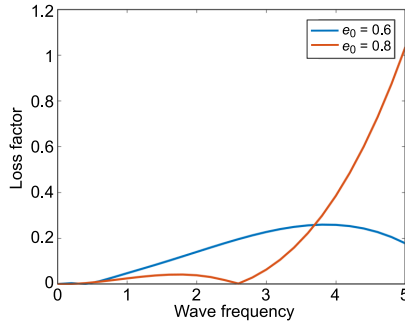


FIG. 10. Variation of loss factor against wave frequency for different e_0 .

Figure 11 exhibits a variation of loss factor against wave frequency with different λ . An increasing loss factor with $\lambda = 0.8$ and $\lambda = 1$ is observed. Figure 12 shows the plot of the internal damping coefficient (τ) in accordance with the

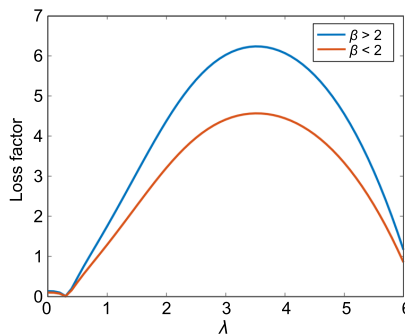


FIG. 11. Variation of loss factor against λ for different β values.

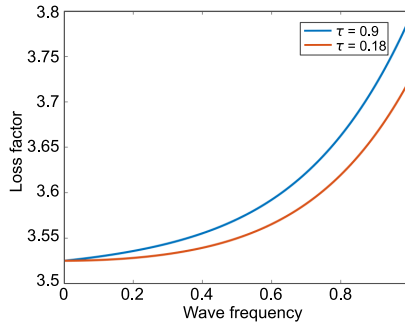


FIG. 12. Variation of loss factor against wave frequency with different τ .

loss factor against the wave frequency. The damping coefficient increases progressively with the increase in the loss factor. Figure 13 shows an increasing damping factor with that of wave number versus wave frequency.

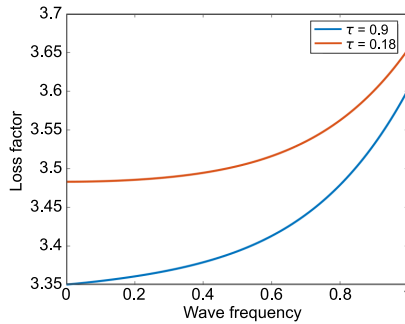


FIG. 13. Variation of wave number against wave frequency with different τ .

7. CONCLUSIONS

The study shows the wave propagation analysis of the piezoelectric FGM nanobeam. The motion of equations of the piezoelectric nanobeam was found by using Hamilton's principle. The governing equations were extracted by substituting the structure displacement field equations into the beam's Euler–Lagrange equations and are framed as symmetric matrices components to arrive at the required solutions. The results of the work are as follows:

- The real and imaginary modes increase when the wave frequency increases, and also imaginary mode is damped at a larger wave frequency.
- The stability behaviors of FGM nanobeam are affected by piezoelectricity.
- Physical variants could be controlled via applying a suitable value of damping factor.

- The greatest loss factor is achieved in the case of zero damping factor and has a linear variation with the wave number.
- Increasing nonlocal values have a significant impact on the loss factor.

REFERENCES

1. KE L.-L., WANG Y.-S., WANG Z.-D., Nonlinear vibration of piezoelectric nanobeams based on the nonlocal theory, *Composite Structures*, **94**(6): 2038–2047, 2012, doi: 10.1016/j.compstruct.2012.01.023.
2. KE L.-L., WANG Y.-S., Thermo electric-mechanical vibration of piezoelectric nanobeams based on the nonlocal theory, *Smart Materials and Structures*, **21**(2): 025018, 2012, doi: 10.1088/0964-1726/21/2/025018.
3. EBRAHIMI F., KHOSRAVI K., DABBAGH A., Wave dispersion in viscoelastic FG nanobeam via a novel spatial-temporal nonlocal strain gradient framework, *Waves in Random and Complex Media*, 2021, doi: 10.1080/17455030.2021.1970282.
4. LAZOPOULOS K.A., LAZOPOULOS A.K., On the fractional deformation of a linearly elastic bar, *Journal of the Mechanical Behavior of Materials*, **29**(1): 9–18, 2020, doi: 10.1515/jmbm-2020-0002.
5. LAZOPOULOS K.A., LAZOPOULOS A.K., On fractional bending of beams, *Archive of Applied Mechanics*, **86**: 1133–1145, 2016, doi: 10.1007/s00419-015-1083-7.
6. ALOTTA G., FAILLA G., ZINGALES M., Finite element formulation of a nonlocal hereditary fractional-order Timoshenko beam, *Journal of Engineering Mechanics*, **143**(5): D4015001, 2017, doi: 10.1061/(ASCE)EM.1943-7889.0001035.
7. SUMELKA W., BLASZCZYK T., LIEBOLD C., Fractional Euler-Bernoulli beams: Theory, numerical study and experimental validation, *European Journal of Mechanics – A/Solids*, **54**: 243–251, 2015, doi: 10.1016/j.euromechsol.2015.07.002.
8. SIDHARDH S., PATNAIK S., SEMPERLOTTI F., Geometrically nonlinear response of a fractional-order nonlocal model of elasticity, *International Journal of Non-Linear Mechanics*, **125**: 103529, 2020, doi: 10.1016/j.ijnonlinmec.2020.103529.
9. STEMPIN P., SUMELKA W., Space-fractional Euler-Bernoulli beam model – Theory and identification for silver nanobeam bending, *International Journal of Mechanical Sciences*, **186**: 105902, 2020, doi: 10.1016/j.ijmecsci.2020.105902.
10. OSKOUIE M.F., ANSARI R., ROUHI H., Bending analysis of functionally graded nanobeams based on the fractional nonlocal continuum theory by the variational Legendre spectral collocation method, *Meccanica*, **53**(4): 1115–1130, 2018, doi: 10.1007/s11012-017-0792-0.
11. ROMANO G., BARRETTA R., Stress-driven versus strain-driven nonlocal integral model for elastic nano-beams, *Composites Part B: Engineering*, **114**: 184–188, 2017, doi: 10.1016/j.compositesb.2017.01.008.
12. BARRETTA R., FABBROCINO F., LUCIANO R., SCIARRA F.M. de, Closed-form solutions in stress-driven two-phase integral elasticity for bending of functionally graded nanobeams, *Physica E: Low-Dimensional Systems and Nanostructures*, **97**: 13–30, 2018, doi: 10.1016/j.physe.2017.09.026.

13. BEDA P.B., Dynamical systems approach of internal length in fractional calculus, *Engineering Transactions*, **65**(1): 209–215, 2017.
14. MOHAMMADI F.S., RAHIMI Z., SUMELKA W., YANG X.-J., Investigation of free vibration and buckling of Timoshenko nano-beam based on a general form of Eringen theory using conformable fractional derivative and Galerkin method, *Engineering Transactions*, **67**(3): 347–367, 2019, doi: 10.24423/EngTrans.1001.20190426.
15. NGUYEN T.-T., KIM N.-I., LEE J., Free vibration of thin-walled functionally graded open-section beams, *Composites Part B: Engineering*, **95**: 105–116, 2016, doi: 10.1016/j.compositesb.2016.03.057.
16. EBRAHIMI F., BARATI M.R., Vibration analysis of smart piezoelectrically actuated nanobeams subjected to magneto-electrical field in thermal environment, *Journal of Vibration and Control*, **24**(3): 549–564, 2018, doi: 10.1177/1077546316646239.
17. ZAOUÏ F.Z., OUINAS D., TOUNSI A., New 2D and quasi-3D shear deformation theories for free vibration of functionally graded plates on elastic foundations, *Composites Part B: Engineering*, **159**: 231–247, 2019, doi: 10.1016/j.compositesb.2018.09.051.
18. ALIBEIGI B., TADI BENI Y., MEHRALIAN F., On the thermal buckling of magneto-electro-elastic piezoelectric nanobeams, *The European Physical Journal Plus*, **133**: 133, 2018, doi: 10.1140/epjp/i2018-11954-7.
19. SHARIATI A., EBRAHIMI F., KARIMIASL M., SELVAMANI R., TOGHROLI A., On bending characteristics of smart magneto-electro-piezoelectric nanobeams system, *Advances in Nano Research*, **9**(3): 183–191, 2020, doi: 10.12989/anr.2020.9.3.183.
20. EBRAHIMI F., KARIMIASL M., SELVAMANI R., Bending analysis of magneto-electro piezo-electric nanobeams system under hygro-thermal loading, *Advances in Nano Research*, **8**(3): 203–214, 2020, doi: 10.12989/anr.2020.8.3.203.
21. EBRAHIMI F., DABBAGH A., *Wave Propagation Analysis of Smart Nanostructures*, CRC Press, 2019, doi: 10.1201/9780429279225.
22. LI S.-R., SU H.-D., CHENG C.-J., Free vibration of functionally graded material beams with surface-bonded piezoelectric layers in thermal environment, *Applied Mathematics and Mechanics*, **30**(8): 969–982, 2009, doi: 10.1007/s10483-009-0803-7.
23. KIANI Y., ESLAMI M.R., Thermal buckling analysis of functionally graded material beams, *International Journal of Mechanics and Materials in Designs*, **6**(3): 229–238, 2010, doi: 10.1007/s10999-010-9132-4.
24. SUN D., LUO S.-N., Wave propagation of functionally graded material plates in thermal environments, *Ultrasonics*, **51**(8): 940–952, 2011, doi: 10.1016/j.ultras.2011.05.009.
25. THAI H.-T., CHOI D.-H., A refined shear deformation theory for free vibration of functionally graded plates on elastic foundation, *Composites Part B: Engineering*, **43**(5): 2335–2347, 2012, doi: 10.1016/j.compositesb.2011.11.062.
26. THAI H.-T., PARK T., CHOI D.-H., An efficient shear deformation theory for vibration of functionally graded plates, *Archive of Applied Mechanics*, **83**(1): 137–149, 2013, doi: 10.1007/s00419-012-0642-4.

27. SHAHSAVARI D., SHAHSAVARI M., LI L., KARAMI B., A novel quasi-3D hyperbolic theory for free vibration of FG plates with porosities resting on Winkler/Pasternak/Kerr foundation, *Aerospace Science and Technology*, **72**: 134–149, 2018, doi: 10.1016/j.ast.2017.11.004.
28. ERINGEN A.C., On differential equations of nonlocal elasticity and solutions of screw dislocation and surface waves, *Journal of Applied Physics*, **54**(9): 4703–4710, 1983, doi: 10.1063/1.332803.
29. CIVALEK Ö., DEMİR Ç., Bending analysis of microtubules using nonlocal Euler–Bernoulli beam theory, *Applied Mathematical Modelling*, **35**(5): 2053–2067, 2011, doi: 10.1016/j.apm.2010.11.004.
30. ARANI A.G., AMIR S., SHAJARI A.R., MOZDIANFARD M.R., Electro-thermo-mechanical buckling of DWBNNTs embedded in bundle of CNTs using nonlocal piezoelectricity cylindrical shell theory, *Composites Part B: Engineering*, **43**(2): 195–203, 2012, doi: 10.1016/j.compositesb.2011.10.012.
31. REDDY J.N., EL-BORGI S., Eringen’s nonlocal theories of beams accounting for moderate rotations, *International Journal of Engineering Science*, **82**: 159–177, 2014, doi: 10.1016/j.ijengsci.2014.05.006.
32. ZHANG L.L., LIU J.X., FANG X.Q., NIE G.Q., Effects of surface piezoelectricity and nonlocal scale on wave propagation in piezoelectric nanoplates, *European Journal of Mechanics – A/Solids*, **46**: 22–29, 2014, doi: 10.1016/j.euromechsol.2014.01.005.
33. NEJAD M.Z., HADI A., Eringen’s non-local elasticity theory for bending analysis of bi-directional functionally graded Euler–Bernoulli nano-beams, *International Journal of Engineering Sciences*, **106**: 1–9, 2016, doi: 10.1016/j.ijengsci.2016.05.005.
34. NEJAD M.Z., HADI A., Non-local analysis of free vibration of bi-directional functionally graded Euler–Bernoulli nano-beams, *International Journal of Engineering Sciences*, **105**: 1–11, 2016, doi: 10.1016/j.ijengsci.2016.04.011.
35. NEJAD M.Z., HADI A., RASTGOO A., Buckling analysis of arbitrary two-directional functionally graded Euler–Bernoulli nano-beams based on nonlocal elasticity theory, *International Journal of Engineering Sciences*, **103**: 1–10, 2016, doi: 10.1016/j.ijengsci.2016.03.001.
36. EBRAHIMI F., BARATI M.R., Size-dependent vibration analysis of viscoelastic nanocrystalline silicon nanobeams with porosities based on a higher order refined beam theory, *Composite Structures*, **166**: 256–267, 2017, doi: 10.1016/j.compstruct.2017.01.036.
37. LIM C.W., ZHANG G., REDDY J.N., A higher-order nonlocal elasticity and strain gradient theory and its applications in wave propagation, *Journal of the Mechanics and Physics of Solids*, **78**: 298–313, 2015, doi: 10.1016/j.jmps.2015.02.001.
38. FARAJPOUR A., HAERI YAZDI M.R., RASTGOO A., MOHAMMADI M., A higher-order nonlocal strain gradient plate model for buckling of orthotropic nanoplates in thermal environment, *Acta Mechanica*, **227**(7): 1849–1867, 2016, doi: 10.1007/s00707-016-1605-6.
39. LI L., LI X., HU Y., Free vibration analysis of nonlocal strain gradient beams made of functionally graded material, *International Journal of Engineering Sciences*, **102**: 77–92, 2016, doi: 10.1016/j.ijengsci.2016.02.010.

40. EBRAHIMI F., DABBAGH A., Wave propagation analysis of embedded nanoplates based on a nonlocal strain gradient-based surface piezoelectricity theory, *The European Physical Journal Plus*, **132**(11): 449, 2017, doi: 10.1140/epjp/i2017-11694-2.
41. HADI A., ZAMANI NEJAD M., HOSSEINI M., Vibrations of three-dimensionally graded nanobeams, *International Journal of Engineering Sciences*, **128**: 12–23, 2018, doi: 10.1016/j.ijengsci.2018.03.004.

Received May 27, 2022; accepted version September 25, 2022.



Copyright © 2022 The Author(s).

This is an open-access article distributed under the terms of the Creative Commons Attribution-ShareAlike 4.0 International (CC BY-SA 4.0 <https://creativecommons.org/licenses/by-sa/4.0/>) which permits use, distribution, and reproduction in any medium, provided that the article is properly cited. In any case of remix, adapt, or build upon the material, the modified material must be licensed under identical terms.